

# Counterrotating perfect fluid discs as sources of electrovacuum static spacetimes

Gonzalo García-Reyes.‡ and Guillermo A. González§

Escuela de Física, Universidad Industrial de Santander, A. A. 678, Bucaramanga, Colombia

**Abstract.** The interpretation of some electrovacuum spacetimes in terms of counterrotating perfect fluid discs is presented. The interpretation is made by means of an “inverse problem” approach used to obtain disc sources of known static solutions of the Einstein-Maxwell equations. In order to do such interpretation, a detailed study is presented of the counterrotating model (CRM) for generic electrovacuum static axially symmetric relativistic thin discs with nonzero radial pressure. Four simple families of models of counterrotating charged discs based on Chazy-Curzon-type, Zipoy-Voorhees-type, Bonnor-Sackfield-type, and charged and magnetized Darmois electrovacuum metrics are considered where we obtain some discs with a CRM well behaved.

Submitted to: *CQG*

PACS numbers: 04.20.-q, 04.20.Jb, 04.40.Nr

## 1. Introduction

Several methods are known to exactly solve the Einstein and Einstein-Maxwell field equations, or to generate new exact solutions from simple known solutions [1]. However, the above mentioned methods in general lead to solutions without a clear physical interpretation or to solutions that depend of many parameters without a clear physical meaning. Accordingly, it is of importance to have some appropriate procedures to obtain physical interpretations of these exact solutions. So, in the past years such procedures have been developed for static and stationary axially symmetric solutions in terms of thin and, more recently, thick disc models.

Stationary or static axially symmetric exact solutions of Einstein equations describing relativistic thin discs are of great astrophysical importance since they can be used as models of certain stars, galaxies and accretion discs. These were first studied by Bonnor and Sackfield [2], obtaining pressureless static discs, and then by Morgan and Morgan, obtaining static discs with and without radial pressure [3, 4]. In connection

‡ e-mail: ggr1970@yahoo.com

§ e-mail: guillego@uis.edu.co

with gravitational collapse, discs were first studied by Chamorro, Gregory, and Stewart [5]. Discs with radial tension have been also studied [6].

Several classes of exact solutions of the Einstein field equations corresponding to static and stationary thin discs have been obtained by different authors, with or without radial pressure (see refs. [7] to [17]). Except for the pressureless disks all the other disks have as source matter with azimuthal pressure (tension) different from the radial pressure (tension). However, in some cases these disks can be interpreted as the superposition of two counterrotating perfect fluids. A detailed study of the counterrotating model for the case of static thin disks is presented in [18]. Recently, more realistic models of thin disks and thin disks with halos made of perfect fluids were considered in [19].

Disc sources for stationary axially symmetric spacetimes with magnetic fields are also of astrophysical importance mainly in the study of neutron stars, white dwarfs and galaxy formation. Although discs with electric fields do not have clear astrophysical importance, their study may be of interest in the context of exact solutions. Thin discs have been discussed as sources for Kerr-Newman fields [20], magnetostatic axisymmetric fields [21], conformastationary metrics [22], and electrovacuum static counterrotating discs [23]. Following Ref. [20] the resulting discs can be interpreted either as rings with internal pressure and currents or as two counterrotating streams of freely moving charged particles, i.e., which move along electrogeodesics (solution to the geodesic equation in the presence of a Lorentz force).

In all the above cases, the discs are obtained by an “inverse problem” approach, called by Synge the “*g-method*” [24]. The method works as follows: a solution of the vacuum Einstein equations is taken, such that there is a discontinuity in the derivatives of the metric tensor on the plane of the disc, and the energy-momentum tensor is obtained from the Einstein equations. The physical properties of the matter distribution are then studied by an analysis of the surface energy-momentum tensor so obtained. Very recently the above procedure has been generalized in order to obtain thick disc models [25] and also non-axisymmetric planar distributions of charged dust [26]. As we can see, by this “inverse problem” approach we can do physical interpretations of many known solutions of the Einstein and Einstein-Maxwell vacuum equations, in the sense that the thin disks can act as exact sources for the space-time metrics given by the vacuum solutions.

The purpose of this paper is the interpretation of some static electrovacuum spacetimes in terms of counterrotating perfect fluid discs. In order to do such interpretation, a detailed study is presented of the counterrotating model (CRM) for generic electrovacuum static axially symmetric relativistic thin discs with nonzero radial pressure. The counterrotating model for the case of static thin discs with radial pressure was recently studied in [18] and for static discs without radial pressure but without electromagnetic field in [23], so the material presented here is a continuation of the mentioned works. The paper is structured as follows. In Sec. 2, we present a summary of the procedure to construct models of discs with nonzero radial pressure. We obtain

expressions for the surface energy-momentum tensor and the surface current density of the disc.

In Sec. 3, the discs are interpreted in terms of the CRM. We find a general constraint over the counterrotating tangential velocities needed to cast the surface energy-momentum tensor of the disc as the superposition of two counterrotating charged perfect fluids. We also find expressions for the energy density, pressure, current density, and tangential velocity of the counterrotating fluids. We show that, in general, it is not possible to take the two counterrotating fluids as circulating along electrogeodesics nor take the two counterrotating tangential velocities as equal and opposite.

In Sec. 4, four simple families of models of counterrotating charged discs based on Chazy-Curzon-type, Zipoy-Voorhees-type, Bonnor-Sackfield-type, and charged and magnetized Darmois metrics are presented where we obtain some discs with a well behaved CRM. In particular, we study the tangential velocities, energy and electric charge densities in the particular case when both streams have equal pressure or equal energy density. Also the stability against radial perturbation is analyzed. Finally, in Sec. 5, we summarize our main results.

## 2. Electrovacuum static relativistic discs

### 2.1. Models of discs with nonzero radial pressure

In this section we present a summary of the procedure to obtain electrovacuum static axially symmetric relativistic thin discs with nonzero radial pressure. The line element of a static axisymmetric field can be written in quasi-cylindrical coordinates  $(t, \varphi, r, z)$  in the form

$$ds^2 = - e^{2\Psi} dt^2 + e^{-2\Psi} [R^2 d\varphi^2 + e^{2\Lambda} (dr^2 + dz^2)] , \quad (1)$$

where  $\Psi$ ,  $\Lambda$  and  $R$  are functions of  $r$  and  $z$  only. The vacuum Einstein-Maxwell equations, in geometrized units in which  $8\pi G = c = \mu_0 = \varepsilon_0 = 1$ , are given by

$$R_{ab} = T_{ab}, \quad (2)$$

$$F^{ab}{}_{;b} = 0, \quad (3)$$

with

$$T_{ab} = F_{ac} F_b{}^c - \frac{1}{4} g_{ab} F_{cd} F^{cd}, \quad (4)$$

$$F_{ab} = \partial_a A_b - \partial_b A_a. \quad (5)$$

In order to obtain a solution of (2) – (3) representing a thin disc at  $z = 0$ , we assume that the components of the metric tensor are continuous across the disc, but with first derivatives discontinuous on the plane  $z = 0$ , with discontinuity functions

$$b_{ab} = g_{ab,z}|_{z=0^+} - g_{ab,z}|_{z=0^-} = 2 g_{ab,z}|_{z=0^+} .$$

Thus, the Einstein-Maxwell equations yield an energy-momentum tensor  $T_{ab} = T_{ab}^{\text{elm}} + T_{ab}^{\text{mat}}$ , where  $T_{ab}^{\text{mat}} = Q_{ab} \delta(z)$ , and a current density  $J_a = j_a \delta(z) = -2e^{2(\Psi-\Lambda)} A_{a,z} \delta(z)$ ,

where  $\delta(z)$  is the usual Dirac function with support on the disk.  $T_{ab}^{\text{elm}}$  is the electromagnetic tensor defined in Eq. (4),  $j_a$  is the current density on the plane  $z = 0$ , and

$$Q_b^a = \frac{1}{2} \{ b^{az} \delta_b^z - b^{zz} \delta_b^a + g^{az} b_b^z - g^{zz} b_b^a + b_c^c (g^{zz} \delta_b^a - g^{az} \delta_b^z) \}$$

is the distributional energy-momentum tensor.

The “true” surface energy-momentum tensor (SEMT) of the disc,  $S_{ab}$ , and the “true” surface current density,  $j_a$ , can be obtained through the relations

$$S_{ab} = \int T_{ab}^{\text{mat}} ds_n = e^{\Lambda - \Psi} Q_{ab}, \quad (6)$$

$$j_a = \int J_a ds_n = e^{\Lambda - \Psi} j_a, \quad (7)$$

where  $ds_n = \sqrt{g_{zz}} dz$  is the “physical measure” of length in the direction normal to the disc. For the metric (1), the nonzero components of  $S_a^b$  are

$$S_0^0 = 2e^{\Psi - \Lambda} \left[ \Lambda_{,z} - 2\Psi_{,z} + \frac{R_{,z}}{R} \right], \quad (8)$$

$$S_1^1 = 2e^{\Psi - \Lambda} \Lambda_{,z}, \quad (9)$$

$$S_2^2 = 2e^{\Psi - \Lambda} \left[ \frac{R_{,z}}{R} \right], \quad (10)$$

and the components of the surface current density are equal to

$$j_t = -2e^{\Psi - \Lambda} \psi_{,z}, \quad (11)$$

$$j_\varphi = -2e^{\Psi - \Lambda} A_{,z}, \quad (12)$$

where  $\psi$  and  $A$  are the electrostatic and magnetostatic potentials, respectively, which are also functions of  $r$  and  $z$  only. All the quantities are evaluated at  $z = 0^+$ .

In order to give physical significance to the components of the energy-momentum tensor  $S_a^b$  we project it onto the orthonormal tetrad  $e_a^b = \{V^b, W^b, X^b, Y^b\}$ , where

$$V^a = e^{-\Psi} (1, 0, 0, 0), \quad X^a = e^{\Psi - \Lambda} (0, 0, 1, 0), \quad (13)$$

$$W^a = \frac{e^\Psi}{R} (0, 1, 0, 0), \quad Y^a = e^{\Psi - \Lambda} (0, 0, 0, 1).$$

In terms of this tetrad (or observer) the metric, the SEMT and the current density may be decomposed as

$$g_{ab} = -V_a V_b + W_a W_b + X_a X_b + Y_a Y_b, \quad (14)$$

$$S_{ab} = \epsilon V_a V_b + p_\varphi W_a W_b + p_r X_a X_b, \quad (15)$$

$$j_a = \sigma V_a + j W_a, \quad (16)$$

where

$$\epsilon = -S_0^0, \quad p_\varphi = S_1^1, \quad p_r = S_2^2, \quad (17)$$

are, respectively, the energy density, the azimuthal pressure, the radial pressure,

$$\sigma = j^0/V^0, \quad j = j^1/W^1, \quad (18)$$

are the electric charge density and the azimuthal current density of the disc measured by this observer with four-velocity  $V^a$ , and

$$\varrho = \epsilon + p_\varphi + p_r \quad (19)$$

is the “effective Newtonian density”.

## 2.2. Solution of the field equations

For the metric (1), the Einstein-Maxwell equations in vacuum imply that  $R$  satisfies the Laplace’s equation

$$R_{,rr} + R_{,zz} = 0, \quad (20)$$

so that the function  $R$  can be considered as the real part of an analytical function  $F(\nu) = R(r, z) + iZ(r, z)$ , where  $\nu = r + iz$ . Thus the function  $F(\nu)$  defines a conformal transformation

$$r \rightarrow R(r, z), \quad z \rightarrow Z(r, z), \quad (21)$$

in such a way that the metric (1) takes the Weyl form

$$ds^2 = -e^{2\mu} dt^2 + e^{-2\mu} [R^2 d\varphi^2 + e^{2\lambda} (dR^2 + dZ^2)], \quad (22)$$

where  $R$  and  $Z$  are the Weyl’s canonical coordinates.

In these coordinates, the field equations (2) – (3) are equivalent to the usual complex Ernst equations [27]

$$f\Delta\mathcal{E} = (\nabla\mathcal{E} + 2\Phi^*\nabla\Phi) \cdot \nabla\mathcal{E}, \quad (23)$$

$$f\Delta\Phi = (\nabla\mathcal{E} + 2\Phi^*\nabla\Phi) \cdot \nabla\Phi, \quad (24)$$

where  $\Delta$  and  $\nabla$  are the standard differential operators in cylindrical coordinates,  $f = e^{2\mu}$  and  $\mathcal{E} = \mathcal{E}^*$  (static spacetime). The metric functions are obtained via

$$f = \mathcal{E} + \Phi\Phi^*, \quad (25)$$

$$\lambda_{,\zeta} = \sqrt{2} \frac{R}{f} \left[ \frac{1}{4f} (\mathcal{E}_{,\zeta} + 2\Phi^*\Phi_{,\zeta})(\mathcal{E}_{,\zeta} + 2\Phi\Phi_{,\zeta}^*) - \Phi_{,\zeta}\Phi_{,\zeta}^* \right], \quad (26)$$

where  $\sqrt{2}\zeta = R + iZ$ , so that  $\sqrt{2}\partial_{,\zeta} = \partial_{,R} - i\partial_{,Z}$ . The electromagnetic potentials are related to  $\Phi$  via

$$A_{\varphi,\zeta} = \sqrt{2}i \frac{R}{f} (\text{Im}\Phi)_{,\zeta}, \quad (27)$$

and  $A_t = \sqrt{2}\text{Re}\Phi$ .

It is known that in static electromagnetic fields there is a lineal relation between the electrostatic potential and its magnetic counterpart [28, 29]. Some authors therefore study only electric fields. In this paper we consider the field equations when both electric and magnetic fields are presents, since the true magnetic potential will be different, and therefore the physical properties will differ too.

Once a solution of the system of equations (23) – (24) is known, we can obtain a solution of the field equations (2) – (3) in the original coordinates by setting

$$R(r, z) = \operatorname{Re}F(\nu), \quad (28)$$

$$\Psi(r, z) = \mu(R, Z), \quad (29)$$

$$\Lambda(r, z) = \lambda(R, Z) + \ln |F'(\nu)|, \quad (30)$$

$$\psi(r, z) = A_t(R, Z), \quad (31)$$

$$A(r, z) = A_\varphi(R, Z), \quad (32)$$

where  $F' = dF/d\nu$ . With this transformation  $p_r$  can be written as

$$p_r = \frac{2e^{\mu-\lambda}}{\sqrt{R_{,r}^2 + R_{,z}^2}} \frac{R_{,z}}{R}. \quad (33)$$

Thus, the construction of thin discs models with nonzero radial pressure depends strongly of the analytical function  $F(\nu)$ , due to the fact that this function gives the behavior of the radial pressure and also defines the conformal transformation that leads the field equations to the form given for Ernst (23) – (24). A common choice for  $F(\nu)$  is

$$F(\nu) = \nu + iz_0, \quad (34)$$

where  $z_0$  is a constant. In this case we have infinite discs with zero radial pressure. This is the well known “displace, cut and reflect” method used in almost all of the works about discs models to generate thin discs from solutions of the Einstein and Einstein-Maxwell equations. Another possible choice for  $F(\nu)$  was presented in reference [6] and is given by

$$F(\nu) = \nu + \alpha\sqrt{\nu^2 - 1}, \quad (35)$$

where  $\alpha \geq 0$ . With this choice for  $F(\nu)$  the general expression for the radial pressure leads to

$$p_r = \frac{2\alpha e^{\mu-\lambda}}{[1 + (\alpha^2 - 1)r^2]^{1/2}}, \quad (36)$$

so that we obtain thin discs with nonzero radial pressure and of finite radius, located at  $z = 0$ ,  $0 \leq r \leq 1$ . In order to obtain discs with non-unit radius, we only need to make the transformation  $r \rightarrow ar$ , where  $a$  is the radius of the disc. We shall also take  $F(\nu)$  as given by (35).

With this choice for  $F(\nu)$  the image of the disc by the conformal mapping (21) is the surface

$$\alpha^2 R^2 + Z^2 = \alpha^2 \quad (37)$$

so that the discs are mapped into spheroidal thin shells of matter and its exterior is mapped into the exterior of the shells. We have three possible values for  $\alpha$ :  $\alpha = 1$ , a spherical shell,  $\alpha > 1$ , a prolate spheroidal shell, and  $0 < \alpha < 1$ , an oblate spheroidal shell. By considering the above shells as sources, we then seek for exterior solutions of the field equations (23) – (24) adapted to the symmetry of the shells. Then, using (28) – (32) we obtain the corresponding disc solutions in the original coordinates.

### 3. The counterrotating model

#### 3.1. Counterrotating charged perfect fluid discs

We now consider, based on Refs. [30] and [31], the possibility that the SEMT  $S^{ab}$  and the current density  $j^a$  can be written as the superposition of two counterrotating charged perfect fluids that circulate in opposite directions; that is, we assume

$$S^{ab} = S_+^{ab} + S_-^{ab}, \quad (38)$$

$$j^a = j_+^a + j_-^a, \quad (39)$$

where the quantities on the right-hand side are, respectively, the SEMT and the current density of the prograde and retrograde counterrotating fluids.

Let  $U_\pm^a = (U_\pm^0, U_\pm^1, 0, 0)$  be the velocity vectors of the two counterrotating fluids. In order to do the decomposition (38) and (39) we project the velocity vectors onto the tetrad  $e_{\hat{a}}{}^b$ , using the relations [32]

$$U_\pm^{\hat{a}} = e^{\hat{a}}{}_b U_\pm^b, \quad U_\pm^a = e_b{}^a U_\pm^{\hat{b}}. \quad (40)$$

In terms of the tetrad (13) we can write

$$U_\pm^a = \frac{V^a + v_\pm W^a}{\sqrt{1 - v_\pm^2}}, \quad (41)$$

where  $v_\pm = U_\pm^1/U_\pm^0$  are the tangential velocities of the streams with respect to the tetrad.

Another quantity related with the counterrotating motion is the specific angular momentum of a particle rotating at a radius  $r$ , defined as  $h_\pm = g_{\varphi\varphi}U_\pm^\varphi$ . We can write

$$h_\pm = \frac{Re^{-\Psi}v_\pm}{\sqrt{1 - v_\pm^2}}. \quad (42)$$

This quantity can be used to analyze the stability of the discs against radial perturbations. The condition of stability,

$$\frac{d(h^2)}{dr} > 0, \quad (43)$$

is an extension of Rayleigh criteria of stability of a fluid in rest in a gravitational field [33].

In terms of the metric  $h_{ab} = g_{ab} - Y_a Y_b$  of the hypersurface  $z = 0$ , we can write the SEMT as

$$S^{ab} = (\epsilon + p_r)V^a V^b + (p_\varphi - p_r)W^a W^b + p_r h^{ab}, \quad (44)$$

and using (41) we obtain

$$\begin{aligned} S^{ab} = & \frac{f(v_-, v_-)(1 - v_+^2) U_+^a U_+^b}{(v_+ - v_-)^2} \\ & + \frac{f(v_+, v_+)(1 - v_-^2) U_-^a U_-^b}{(v_+ - v_-)^2} \end{aligned}$$

$$\begin{aligned}
 & - \frac{f(v_+, v_-)(1 - v_+^2)^{\frac{1}{2}}(1 - v_-^2)^{\frac{1}{2}}(U_+^a U_-^b + U_-^a U_+^b)}{(v_+ - v_-)^2} \\
 & + p_r h^{ab},
 \end{aligned}$$

where

$$f(v_+, v_-) = (\epsilon + p_r)v_+v_- + p_\varphi - p_r. \quad (45)$$

Clearly, in order to cast the SEMT in the form (38), the mixed term must be absent and therefore the counterrotating tangential velocities must be related by

$$f(v_+, v_-) = 0, \quad (46)$$

where we assume that  $|v_\pm| \neq 1$ .

Then, assuming a given choice for the tangential velocities in agreement with the above relation, we can write the SEMT as (38) with

$$S_\pm^{ab} = (\epsilon_\pm + p_\pm) U_\pm^a U_\pm^b + p_\pm h^{ab}, \quad (47)$$

so that we have two counterrotating perfect fluids with energy densities and pressures, measured by an observer comoving with the streams, given by

$$\epsilon_\pm + p_\pm = \left[ \frac{1 - v_\pm^2}{v_\mp - v_\pm} \right] (\epsilon + p_r)v_\mp, \quad (48)$$

$$p_+ + p_- = p_r. \quad (49)$$

From these equations also follows that

$$\epsilon_+ + \epsilon_- = \epsilon + p_r - p_\varphi. \quad (50)$$

Thus the SEMT  $S^{ab}$  can be written as the superposition of two counterrotating perfect fluids if, and only if, the constraint (46) admits a solution such that  $v_+ \neq v_-$ . This result is completely equivalent to the necessary and sufficient condition obtained in Ref. [31].

Similarly, substituting (41) in (16) we can write the current density as (39) with

$$j_\pm^a = \sigma_\pm U_\pm^a, \quad (51)$$

where  $\sigma_\pm$  are the counterrotating electric charge densities measured by an observer comoving with the streams, which are given by

$$\sigma_\pm = \left[ \frac{\sqrt{1 - v_\pm^2}}{v_\pm - v_\mp} \right] (j - \sigma v_\mp). \quad (52)$$

Thus, we have a disc made of two counterrotating charged perfect fluids with energy densities and pressures given by (48) and (49), and electric charge densities given by (52).

### 3.2. Counterrotating tangential velocities

All the main quantities associated with the CRM depend on the counterrotating tangential velocities  $v_{\pm}$ . However, even for known values of  $v_{\pm}$ , the system of equations (48) – (49) is underdetermined so that we can have information about the physical quantities corresponding to each stream only in some particular situations. We will examine two simple cases in this paper, when the two streams have equal pressure and when they have equal energy density. On the other hand, the constraint (46) does not determine  $v_{\pm}$  uniquely so that we need to impose some additional requirement in order to obtain a complete determination of the tangential velocities leading to a well defined CRM.

A possibility, commonly assumed, is to take the two counterrotating streams as circulating along electrogeodesics

$$\frac{1}{2}\epsilon_{\pm}g_{ab,r}U_{\pm}^aU_{\pm}^b = -\sigma_{\pm}F_{ra}U_{\pm}^a. \quad (53)$$

Let  $\omega_{\pm} = U_{\pm}^1/U_{\pm}^0$  be the angular velocities of the particles. In terms of  $\omega_{\pm}$  (53) takes the form

$$\frac{1}{2}\epsilon_{\pm}(g_{11,r}\omega_{\pm}^2 + g_{00,r}) = -\sigma_{\pm}\frac{1}{U_{\pm}^0}(\psi_{,r} + A_{,r}\omega_{\pm}), \quad (54)$$

and  $v_{\pm}$  can be written as

$$v_{\pm} = \left[ \frac{V^0}{W^1} \right] \omega_{\pm}. \quad (55)$$

As an example, let us consider the electrogeodesic motion of the particles when we have equal energy density. By simplicity, we will analyze the electrostatic and magnetostatic cases separately. The angular velocity  $\omega_{\pm}$  can be obtained from the electrogeodesic equation (54) and, in the electrostatic case, we obtain  $\omega_{\pm} = \pm\omega$  with

$$\omega^2 = \frac{e^{4\Psi}}{R} \left[ \frac{-2\Psi_{,r}(\Psi_{,z} - \Lambda_{,z}) + \psi_{,r}\psi_{,z}e^{-2\Psi}}{-2(\Psi_{,z} - \Lambda_{,z})(R_{,r} - R\Psi_{,r}) + R\psi_{,r}\psi_{,z}e^{-2\Psi}} \right], \quad (56)$$

and therefore

$$f(v_+, v_-) = -R \left[ \frac{2(\Psi_{,z} - \Lambda_{,z})dp_r/dr + p_r\psi_{,r}\psi_{,z}e^{-2\Psi}}{-2(\Psi_{,z} - \Lambda_{,z})(R_{,r} - R\Psi_{,r}) + R\psi_{,r}\psi_{,z}e^{-2\Psi}} \right], \quad (57)$$

where we have used the Einstein-Maxwell equations (2) and (3) for  $\Lambda$  and the expressions (8) - (12) for the SEMT and the current density. It follows immediately that  $f(v_+, v_-)$  vanishes if

$$\frac{1}{p_r} \frac{dp_r}{dr} = -\frac{\psi_{,r}\psi_{,z}e^{-2\Psi}}{2(\Psi_{,z} - \Lambda_{,z})}, \quad (58)$$

and therefore

$$p_r = c_1 e^{f_1(r)}, \quad (59)$$

where  $c_1$  is a constant and

$$f_1(r) = -\int \frac{\psi_{,r}\psi_{,z}e^{-2\Psi}}{2(\Psi_{,z} - \Lambda_{,z})} dr. \quad (60)$$

Similarly, for magnetostatic fields we obtain again  $\omega_{\pm} = \pm\omega$  with

$$\omega^2 = e^{4\Psi} \left[ \frac{2\Psi_{,r}(\Psi_{,z} - \Lambda_{,z}) + A_{,r}A_{,z}e^{2\Psi}/R^2}{2R(\Psi_{,z} - \Lambda_{,z})(R_{,r} - R\Psi_{,r}) + A_{,r}A_{,z}e^{2\Psi}} \right], \quad (61)$$

so that

$$f(v_+, v_-) = R \left[ \frac{2(\Psi_{,z} - \Lambda_{,z})dp_r/dr - p_r A_{,r}A_{,z}e^{2\Psi}}{-2(\Psi_{,z} - \Lambda_{,z})(R_{,r} - R\Psi_{,r}) + A_{,r}A_{,z}e^{2\Psi}/R} \right]. \quad (62)$$

That is,  $f(v_+, v_-)$  vanishes if

$$\frac{1}{p_r} \frac{dp_r}{dr} = \frac{A_{,r}A_{,z}e^{2\Psi}}{2(\Psi_{,z} - \Lambda_{,z})}, \quad (63)$$

and therefore

$$p_r = c_2 e^{f_2(r)}, \quad (64)$$

where again  $c_2$  is a constant and

$$f_2(r) = \int \frac{A_{,r}A_{,z}e^{2\Psi}}{2(\Psi_{,z} - \Lambda_{,z})} dr. \quad (65)$$

That is, for electrostatic or magnetostatic fields and equal energy densities the streams circulate along electrogeodesics only if the radial pressure satisfies (59) or (64), respectively. Note that the two electrogeodesic fluids are circulating with equal and opposite tangential velocities. In more general situations, for example with simultaneous presence of electric and magnetic fields,  $p_r$  is a complicated function of  $r$  that can be obtained by a similar procedure and the streams would move with different velocities.

As we can see, in order to have the counterrotating fluids circulating along electrogeodesics, the radial pressure must satisfy a very strong condition that, in general, is not satisfied by the thin disc solutions. Accordingly, we need to consider an additional requirement different of the electrogeodesic motion in order to exactly determine the counterrotating velocities. Another possibility is to take the particles of the streams not circulating along electrogeodesics but with equal and opposite tangential velocities, that is

$$v_{\pm} = \pm v, \quad (66)$$

so that (46) is equivalent to

$$v^2 = \left[ \frac{p_{\varphi} - p_r}{\epsilon + p_r} \right]. \quad (67)$$

This choice, commonly considered, leads to a complete determination of the velocity vectors. However, this can be made only when the above expression is positive definite. In particular, when the two streams have equal pressure or equal energy density we have  $p_{\pm} = \frac{1}{2}p_r$  and  $\epsilon_{\pm} = \frac{1}{2}(\epsilon + p_r - p_{\varphi})$ .

In the general case, when (67) is not positive definite, the two fluids circulate with different velocities and we can write (46) as

$$v_+ v_- = \left[ \frac{p_r - p_{\varphi}}{\epsilon + p_r} \right], \quad (68)$$

and so we can obtain a CRM only if

$$|p_r - p_\varphi| < |\epsilon + p_r|. \quad (69)$$

However, this relation does not determine completely the tangential velocities, and therefore the CRM is undetermined.

#### 4. Some simple examples of counterrotating charged discs

##### 4.1. Discs from a Chazy-Curzon-type solution

The first family of solutions to consider is a Chazy-Curzon-type solution which is given by

$$e^\mu = \frac{2}{(a+1)e^{\gamma/\rho} - (a-1)e^{-\gamma/\rho}}, \quad (70)$$

$$\lambda = -\frac{\gamma^2 \sin^2 \theta}{2\rho^2}, \quad (71)$$

$$A_t = \frac{\sqrt{2}q_1[e^{\gamma/\rho} - e^{-\gamma/\rho}]}{(a+1)e^{\gamma/\rho} - (a-1)e^{-\gamma/\rho}}, \quad (72)$$

$$A_\varphi = \sqrt{2}\gamma q_2 \cos \theta, \quad (73)$$

where  $a^2 = 1 + b^2$ , with  $b^2 = q_1^2 + q_2^2$ , and  $\gamma$  is a real constant. Here  $q_1$  and  $q_2$  are the electric and magnetic parameters, respectively.  $\rho$  and  $\theta$  are quasi-spherical coordinates, related to the Weyl coordinates by

$$R = \rho \sin \theta, \quad Z = \rho \cos \theta, \quad (74)$$

where  $0 \leq \rho \leq \infty$  and  $-\frac{\pi}{2} \leq \theta \leq \frac{\pi}{2}$ . In this coordinates we must choose  $\alpha = 1$  and the shell would be located at  $\rho = 1$ . This solution can be generated, in these coordinates, using the well-known complex potential formalism proposed by Ernst [27] from the Chazy-Curzon vacuum solution [34, 35], by choosing the parameter  $q$  of Ref. [27] as complex. For  $q_2 = 0$  we have an electrostatic solution and for  $q_1 = 0$  one obtains its magnetostatic analogue [36].

From the above expressions we can compute the physical quantities associated with the discs. We obtain

$$\epsilon = \varrho - p_r - p_\varphi, \quad (75)$$

$$p_\varphi = p_r(1 + \gamma^2 r^2), \quad (76)$$

$$p_r = p_0 e^{\gamma^2 r^2/2}, \quad (77)$$

$$\sigma = -\frac{q_1 p_0}{\sqrt{2}} p_r, \quad (78)$$

where

$$p_0 = \frac{4}{(a+1)e^\gamma - (a-1)e^{-\gamma}} \quad (79)$$

is a constant and

$$\varrho = \frac{\gamma p_0}{2} [(a+1)e^\gamma + (a-1)e^{-\gamma}] p_r. \quad (80)$$

The strong energy condition requires that  $\rho \geq 0$ , so that we must choose  $\gamma > 0$ . We can see that  $p_0$  is a positive constant for these values of  $\gamma$ .

In order to study the behavior of these quantities we perform a graphical analysis of them for discs with  $\gamma = 2$  and different values of  $q_1$  and  $q_2$ , as functions of  $r$ . In Figs. 1(a) and 1(b) we show the energy density and the pressures  $p_r$  and  $p_\varphi$  for  $q_1 = q_2 = 0, 0.5, 1.0, \text{ and } 1.5$ . We see that the energy density initially is a positive quantity and then becomes negative in violation of the weak energy condition. Therefore only the central region of these discs has a physically reasonable behavior. We can observe that the pressures  $p_r$  and  $p_\varphi$  are always positive quantities everywhere on discs. We also see that the presence of electromagnetic field diminishes the energy density near to the center of the discs and later increases it, and it diminishes the pressures everywhere on discs. Next, the charge density  $\sigma$  is represented in Fig. 1(c) for  $q_1 = q_2 = 0, 0.2, 0.3, 0.5, \text{ and } 1.5$ . As we can see, it exhibits a similar behavior to the radial pressure. We also computed these functions for other values of the parameters (with  $\gamma > 0$ ) and, in all the cases, we found a similar behavior.

We now consider the CRM. All the significant quantities can also be expressed in analytic form from the above expressions but the results are so cumbersome that better turns out only to analyze them graphically. Let us consider the case when the two fluids move with equal and opposite tangential velocities. In Fig. 1(d) we plot the tangential velocity curves of the counterrotating streams  $v^2$  for discs with  $\gamma = 0.7$  and  $q_1 = q_2 = 2, 3, 5, \text{ and } 10$ . We see that the inclusion of electromagnetic field can make the velocities of the particles smaller than the light velocity. In Fig. 1(e) we have drawn the angular momentum  $h^2$  for the same values of the parameters. In some cases we have strong changes in the slope at certain value of  $r$ , which means that there is a strong instability there. For other values of the parameters  $h^2$  is an increasing monotonous function of  $r$  that corresponds to a stable CRM for the discs. Finally, in Fig. 1(f) we have plotted the energy and electric charge densities  $\epsilon_\pm$  and  $\sigma_\pm$  in the particular case when the two streams have equal pressure or equal energy density, for values of the parameters for which  $v^2 < 1$ . We see that  $\sigma_\pm$  behaves in the opposite way to  $\sigma$ , whereas  $\epsilon_\pm$  has a similar behavior to the energy density  $\epsilon$ . Therefore, for Chazy-Curzon-type fields we can build counterrotating thin disc sources only with a well-behaved central region.

#### 4.2. Discs from a Zipoy-Voorhees-type solution

The second family of solutions considered is a Zipoy-Voorhees-type solution which can be written as

$$e^\mu = \frac{2(x^2 - 1)^{\gamma/2}}{(a + 1)(x + 1)^\gamma - (a - 1)(x - 1)^\gamma}, \quad (81)$$

$$\lambda = \frac{\gamma^2}{2} \ln \left[ \frac{x^2 - 1}{x^2 - y^2} \right], \quad (82)$$

$$A_t = \frac{\sqrt{2}q_1[(x + 1)^\gamma - (x - 1)^\gamma]}{(a + 1)(x + 1)^\gamma - (a - 1)(x - 1)^\gamma}, \quad (83)$$

$$A_\varphi = \sqrt{2}k\gamma q_2 y, \quad (84)$$

where  $a^2 = 1 + b^2$ , with  $b^2 = q_1^2 + q_2^2$ , and  $\gamma$  is a real constant. Here  $q_1$  and  $q_2$  are again the electric and magnetic parameters, respectively.  $x$  and  $y$  are the prolate spheroidal coordinates, related to the Weyl coordinates by

$$R^2 = k^2(x^2 - 1)(1 - y^2), \quad Z = kxy, \quad (85)$$

where  $1 \leq x \leq \infty$  and  $0 \leq y \leq 1$ . In this case we must choose  $\alpha > 1$  and the shell would be located at  $x = \alpha/k > 1$  and  $y = \sqrt{1 - r^2}$ , with  $k = \sqrt{\alpha^2 - 1}$ .

This solution can also be generated, in these coordinates, using the well-known complex potential formalism proposed by Ernst [27] from the Zipoy-Voorhees vacuum solution [37, 38], also known as the Weyl  $\gamma$ -solution [39, 40], by choosing the parameter  $q$  of Ref. [27] as complex. For  $q_2 = 0$  we also have an electrostatic solution and for  $q_1 = 0$  one obtains its magnetostatic equivalent [36]. The case  $q_2 = 0$  and  $\gamma = 1$  corresponds to the Reissner-Nordström solution [1], in which case  $a = m/k$ ,  $q_1 = e/k$ , with  $k^2 = m^2 - e^2$ , so that  $a^2 = 1 + q_1^2$ ,  $m$  and  $e$  being the mass and charge parameters, respectively. When  $q_1 = 0$  and  $\gamma = 2$  one arrives to a Taub-NUT-type magnetostatic solution. This solution can also be generated, in these coordinates, using a well-known theorem proposed by Bonnor (see Ref. [42]) from the Taub-NUT vacuum solution. Note that for  $b = 0$ , it reduces to the Darmois metric [1].

From the above expressions we can compute the physical quantities associated with the discs. We obtain

$$\epsilon = \varrho - p_r - p_\varphi, \quad (86)$$

$$p_\varphi = \left[ \frac{1 + k^2\gamma^2 r^2}{1 + k^2 r^2} \right] p_r, \quad (87)$$

$$p_r = p_0 [1 + k^2 r^2]^{\frac{1}{2}(\gamma^2 - 1)}, \quad (88)$$

$$\sigma = - \frac{\gamma k q_1 p_0}{\sqrt{2}\alpha^2} p_r, \quad (89)$$

where

$$p_0 = \frac{4\alpha}{(a+1)(\alpha+k)^\gamma - (a-1)(\alpha-k)^\gamma} \quad (90)$$

is a constant and

$$\varrho = \frac{\gamma k p_0}{2\alpha^2} [(a+1)(\alpha+k)^\gamma + (a-1)(\alpha-k)^\gamma] p_r. \quad (91)$$

Again we must choose  $\gamma > 0$  so that  $\varrho \geq 0$  and the solution satisfies the strong energy condition.  $p_0$  is also a positive constant for these values of  $\gamma$ .

In Figs. 2(a) – 2(c) the plots of the quantities  $\epsilon$ ,  $p_\varphi$ ,  $p_r$ , and  $\sigma$  are presented for discs with  $\alpha = 3$ ,  $\gamma = 1.2$ , and  $q_1 = q_2 = 0, 0.5, 0.8$ , and  $1.5$ , as functions of  $r$ . As in the previous case, we see that the energy density initially is a positive quantity and then becomes negative in violation of the weak energy condition. Therefore only the central region of these discs has a physically reasonable behavior. The another functions also have a similar behavior to the precedent case. We also study Zipoy-Voorhees-type discs for other values of the parameters, but in all the cases we found a similar behavior.

In the same way, the relevant quantities of the CRM are shown in the following figures for the same values of the parameters, also as functions of  $r$ . We also consider the case when the two fluids move with equal and opposite tangential velocities. Here the tangential velocity  $v^2$  (Fig. 2(d)) is always less than the light velocity. One also finds that the inclusion of electromagnetic field makes less relativistic these discs. We also obtain  $h^2$  (Fig. 2(e)) always as an increasing monotonous function of  $r$  that corresponds to a stable CRM for the discs. Finally, in Fig. 2(f) we have plotted the energy and electric charge densities  $\epsilon_{\pm}$  and  $\sigma_{\pm}$  in the particular case when the two streams have equal pressure or equal energy density. We see that  $\sigma_{\pm}$  has a similar behavior to  $\sigma$ , and  $\epsilon_{\pm}$  to the energy density  $\epsilon$ . Therefore, for Zipoy-Voorhees-type fields we can build counterrotating thin disc sources only with a well-behaved central region.

#### 4.3. Discs from a Bonnor-Sackfield-type solution

The third family of solutions considered is a Bonnor-Sackfield-type solution which is given by

$$e^{\mu} = \frac{2}{(a+1)e^{\gamma \cot^{-1} u} - (a-1)e^{-\gamma \cot^{-1} u}}, \quad (92)$$

$$\lambda = -(\gamma^2/2) \ln \left[ (u^2 + 1)/(u^2 + w^2) \right], \quad (93)$$

$$A_t = \frac{\sqrt{2}q_1 [e^{\gamma \cot^{-1} u} - e^{-\gamma \cot^{-1} u}]}{(a+1)e^{\gamma \cot^{-1} u} - (a-1)e^{-\gamma \cot^{-1} u}}, \quad (94)$$

$$A_{\varphi} = \sqrt{2}k\gamma q_2 w, \quad (95)$$

where  $a^2 = 1 + b^2$ , with  $b^2 = q_1^2 + q_2^2$ , and  $\gamma$  is a real constant. Here  $q_1$  and  $q_2$  are again the electric and magnetic parameters, respectively.  $u$  and  $w$  are the oblate spheroidal coordinates, related to the Weyl coordinates by

$$R^2 = k^2(u^2 + 1)(1 - w^2), \quad Z = kuw, \quad (96)$$

where  $0 \leq u \leq \infty$  and  $0 \leq w \leq 1$ . In this case we must choose  $0 < \alpha < 1$  and the shell would be located at  $u = \alpha/k > 0$  and  $w = \sqrt{1 - r^2}$ , with  $k = \sqrt{1 - \alpha^2}$ . As in the precedent cases this solution can be generated, in these coordinates, following Ernst's method [27] from the Bonnor-Sackfield vacuum solution [2].

From the above expressions we can compute the physical quantities associated with the discs. We obtain

$$\epsilon = \varrho - p_r - p_{\varphi}, \quad (97)$$

$$p_r = p_0 [1 - k^2 r^2]^{-(\gamma^2 + 1)/2} \quad (98)$$

$$p_{\varphi} = \left[ \frac{1 + k^2 \gamma^2 r^2}{1 - k^2 r^2} \right] p_r, \quad (99)$$

$$\sigma = -\frac{\gamma k q_1 p_0}{\sqrt{2} \alpha^2} p_r, \quad (100)$$

where

$$p_0 = \frac{4\alpha}{(a+1)e^{\gamma \cot^{-1} u} - (a-1)e^{-\gamma \cot^{-1} u}} \quad (101)$$

is a constant and

$$\varrho = \frac{\gamma k p_0}{2\alpha^2} \left[ (a+1)e^{\gamma \cot^{-1} u} + (a-1)e^{-\gamma \cot^{-1} u} \right] p_r. \quad (102)$$

Here we also must choose  $\gamma > 0$  so that  $\varrho \geq 0$  and the solution satisfies the strong energy condition.  $p_0$  is also a positive constant for these values of  $\gamma$ .

In Figs. 3(a) – 3(c) the plots of the above quantities are presented for discs with  $\alpha = 0.5$ ,  $\gamma = 1.3$ , and  $q_1 = q_2 = 0, 0.5, 0.8$ , and  $1.5$ , as functions of  $r$ . As in the previous cases, we see that the energy density initially is a positive quantity and then becomes negative in violation of the weak energy condition. Therefore only the central region of these discs has a physically reasonable behavior. The another functions also have a similar behavior to the earlier cases. We also study Bonnor-Sackfield-type discs for other values of the parameters, but in all the cases we found a similar behavior.

Again, the relevant quantities of the CRM are shown in the following figures, also as functions of  $r$ . We also consider the case when the two fluids move with equal and opposite tangential velocities. Here the tangential velocity  $v^2$  (Fig. 3(d)) is not always less than the light velocity. However the inclusion of electromagnetic field can make the velocities of the particles smaller than the light velocity. In some cases  $h^2$  (Fig. 3(e)) presents strong changes in the slope at certain value of  $r$ , which means that there is a strong instability there. For other values of the parameters  $h^2$  is an increasing monotonous function of  $r$  that corresponds to a stable CRM for the discs.

Finally, in Fig. 3(f) we have plotted the energy and electric charge densities  $\epsilon_{\pm}$  and  $\sigma_{\pm}$  in the particular case when the two streams have equal pressure or equal energy density. We see that  $\epsilon_{\pm}$  has a similar behavior to the energy density  $\epsilon$ . Therefore, for Bonnor-Sackfield-type fields we can build counterrotating thin disc sources only with a well-behaved central region.

#### 4.4. Discs from a charged and magnetized Darmois solution

Finally, other family of solutions to the Einstein-Maxwell equations is a charged and magnetized Darmois solution, which is given by

$$e^{\mu} = \frac{a^2 x^2 - b^2 y^2 - 1}{(ax + 1)^2 - b^2 y^2}, \quad (103)$$

$$\lambda = 2 \ln \left[ \frac{a^2 x^2 - b^2 y^2 - 1}{a^2 (x^2 - y^2)} \right], \quad (104)$$

$$A_t = \frac{2\sqrt{2}q_1 y}{(ax + 1)^2 - b^2 y^2}, \quad (105)$$

$$A_{\varphi} = - \frac{\sqrt{2}kq_2(1 - y^2)(ax + 1)}{a(a^2 x^2 - b^2 y^2 - 1)}, \quad (106)$$

where  $a^2 = 1 + b^2$ , with  $b^2 = q_1^2 + q_2^2$ . Here  $q_1$  and  $q_2$  are also the electric and magnetic parameters, respectively.  $x$  and  $y$  are the prolate spheroidal coordinates, given by (85). Again we must choose  $\alpha > 1$  and the shell would be located at  $x = \alpha/k > 1$  and  $y = \sqrt{1 - r^2}$ , with  $k = \sqrt{\alpha^2 - 1}$ . For  $b = 0$  this solution also reduces to the

Darmois metric. Moreover, for  $q_2 = 0$  we have a Kerr-type electrostatic solution. This solution can be generated, in these coordinates, using a well-known theorem proposed by Bonnor (see Ref. [42]) from the Kerr vacuum solution. And for  $q_1 = 0$  one obtains its magnetostatic equivalent. This solution is asymptotically flat and was first studied by Bonnor [43] in a different system of coordinates and describes the field of a massive magnetic dipole.

The physical quantities associated with the discs can now be written as

$$\epsilon = \varrho - p_r - p_\varphi, \quad (107)$$

$$p_\varphi = \left[ \frac{a^2 + k^2(4 + b^2)r^2}{(1 + k^2r^2)(a^2 + k^2b^2r^2)} \right] p_r, \quad (108)$$

$$p_r = \frac{2\alpha a^4(1 + k^2r^2)^{3/2}}{(a^2 + k^2b^2r^2)[(\alpha a + k)^2 - k^2b^2(1 - r^2)]}, \quad (109)$$

$$\sigma = - \left[ \frac{4\sqrt{2}a q_1(\alpha a + k)(1 - r^2)^{1/2}}{\alpha(a^2 + k^2b^2r^2)[(\alpha a + k)^2 - k^2b^2(1 - r^2)]} \right] p_r, \quad (110)$$

$$j = - \left[ \frac{\sqrt{2}q_2kr^2}{4a} \right] \varrho, \quad (111)$$

where

$$\varrho = \frac{4ak}{\alpha(a^2 + k^2b^2r^2)} \left[ \frac{(\alpha a + k)^2 + k^2b^2(1 - r^2)}{(\alpha a + k)^2 - k^2b^2(1 - r^2)} \right] p_r. \quad (112)$$

In Figs. 4(a) – 4(c) the plots of the above quantities are shown for discs with  $\alpha = 1.5$  and  $q_1 = q_2 = 0, 0.5, 1.0,$  and  $1.5$ , as functions of  $r$ . We see that these discs also have a central region well behaved which satisfies the weak and strong energy conditions and border region where  $\epsilon < 0$ , in violation of the weak energy condition. We also computed these functions for other values of the parameters, but in all the cases we found a similar behavior.

Equally, the relevant quantities of the CRM are shown in the following figures, also as functions of  $r$ . We also consider the case when the two fluids move with equal and opposite tangential velocities. We see that the inclusion of electromagnetic field can make the velocities of the particles smaller than the light velocity. Here  $v^2$  [Fig. 4(d)] can also take negative values. In some cases  $h^2$  [Fig. 4(e)] presents strong changes in the slope at certain values of  $r$ , which means that we have a strong instability there, and also we find regions with negative slope, showing that the CRM can not be applied for these values of the parameters. However for  $q_1 = q_2 = 0.7$   $h^2$  is always an increasing monotonous function of  $r$  that corresponds to a stable CRM for this disc.

Finally, in Fig. 4(f) we have plotted  $\epsilon_\pm$ ,  $\sigma_+$ , and  $\sigma_-$  in the particular case when the two streams have equal pressure or equal energy density, for values of the parameters for which  $v^2 < 1$ . We see that  $\epsilon_\pm$  has a similar behavior to the energy density  $\epsilon$ . Therefore, for this solution we can build counterrotating thin disc sources only with a well-behaved central region.

## 5. Discussion

A detailed study was presented of the counterrotating model for generic electrovacuum static axially symmetric relativistic thin discs with nonzero radial pressure. A general constraint over the counterrotating tangential velocities was found, needed to cast the surface energy-momentum tensor of the disc in such a way that it can be interpreted as the superposition of two counterrotating charged perfect fluids. The constraint found is completely equivalent to the necessary and sufficient condition obtained in Ref. [31]. We show that, in general, it is not possible to take the two counterrotating fluids as circulating along electrogeodesics neither take the two counterrotating tangential velocities as equal and opposite. We also have obtained explicit expressions for the energy densities, current densities, and velocities of the counterrotating streams in terms of the energy density, azimuthal pressure, and planar current density of the discs, that are also equivalent to the corresponding expressions in Ref. [31].

Four families of models of counterrotating charged discs were considered in the present work based on simple solutions to the vacuum Einsteins-Maxwell equations in the static axisymmetric case generated by conventional solution-generating techniques [1]. We saw that the presence of an electromagnetic field can make the counterrotating tangential velocities of the particles smaller than the light velocity, and also can stabilize against radial perturbations the CRM. The discs constructed have a well-behaved central region which satisfies the weak and strong energy conditions and border region where the energy density is negative, in violation of the weak energy condition.

Finally, the generalization of the counterrotating model presented here to the case of rotating thin discs with or without radial pressure in presence of electromagnetic fields is being considered.

## Acknowledgments

The authors want to thank the financial support from COLCIENCIAS, Colombia. G.G.R. also wants to thank the the Centro Nacional de Cálculo Científico, Universidad de los Andes, Venezuela, for financial support, and the warm hospitality of the Centro de Astrofísica Teórica, Universidad de los Andes, Venezuela, where part of this work was performed.

## References

- [1] D. Kramer, H. Stephani, E. Herlt, and M. McCallum, *Exact Solutions of Einsteins's Field Equations* (Cambridge University Press, Cambridge, England, 1980).
- [2] W. A. Bonnor and A. Sackfield, *Commun. Math. Phys.* **8**, 338 (1968).
- [3] T. Morgan and L. Morgan, *Phys. Rev.* **183**, 1097 (1969).
- [4] L. Morgan and T. Morgan, *Phys. Rev. D* **2**, 2756 (1970).
- [5] A. Chamorro, R. Gregory, and J. M. Stewart, *Proc. R. Soc. London* **A413**, 251 (1987).
- [6] G. A. González and P. S. Letelier, *Class. Quantum Grav.* **16**, 479 (1999).
- [7] D. Lynden-Bell and S. Pineault, *Mon. Not. R. Astron. Soc.* **185**, 679 (1978).

- [8] P.S. Letelier and S. R. Oliveira, *J. Math. Phys.* **28**, 165 (1987).
- [9] J. P. S. Lemos, *Class. Quantum Grav.* **6**, 1219 (1989).
- [10] J. P. S. Lemos and P. S. Letelier, *Class. Quantum Grav.* **10**, L75 (1993).
- [11] J. Bičák, D. Lynden-Bell, and J. Katz, *Phys. Rev. D* **47**, 4334 (1993).
- [12] J. Bičák, D. Lynden-Bell, and C. Pichon, *Mon. Not. R. Astron. Soc.* **265**, 126 (1993).
- [13] J. Bičák and T. Ledvinka, *Phys. Rev. Lett.* **71**, 1669 (1993).
- [14] J. P. S. Lemos and P. S. Letelier, *Phys. Rev. D* **49**, 5135 (1994).
- [15] J. P. S. Lemos and P. S. Letelier, *Int. J. Mod. Phys. D* **5**, 53 (1996).
- [16] C. Klein, *Class. Quantum Grav.* **14**, 2267 (1997).
- [17] G. A. González and P. S. Letelier, *Phys. Rev. D* **62**, 064025 (2000).
- [18] G.A. González and O.A. Espitia, *Phys. Rev. D* **68**, 104028 (2003).
- [19] D. Vogt and P. S. Letelier, *Phys. Rev. D* **68**, 084010 (2003).
- [20] T. Ledvinka, J. Bičák, and M. Žofka, in *Proceeding of 8th Marcel-Grossmann Meeting in General Relativity*, edited by T. Piran (World Scientific, Singapore, 1999)
- [21] P. S. Letelier, *Phys. Rev. D* **60**, 104042 (1999).
- [22] J. Katz, J. Bičák, and D. Lynden-Bell, *Class. Quantum Grav.* **16**, 4023 (1999).
- [23] G. García R. and G. A. González, *Phys. Rev. D* **69**, 124002 (2004).
- [24] J. L. Synge, *Relativity: The General Theory*. (North-Holland, Amsterdam, 1966).
- [25] G. A. González and P. S. Letelier, *Phys. Rev. D* **69**, 044013 (2004).
- [26] D. Vogt and P. S. Letelier, *Class. Quantum Grav.* **21**, 3369 (2004).
- [27] F.J. Ernst, *Phys. Rev. D* **168**, 1415 (1968).
- [28] Z. Perjés, *Nuovo Cim. B* **55**, 600 (1968)
- [29] A. Das, *J. Math. Phys.* **20**, 740 (1979)
- [30] P.S. Letelier, *Phys. Rev. D* **22**, 807 (1980).
- [31] J.J. Ferrando, J.A. Morales, and M. Portilla, *Gen. Relativ. Gravit.* **22**, 1021 (1990).
- [32] S. Chandrasekar, *The Mathematical Theory of Black Holes*. (Oxford University Press, New York, 1992).
- [33] L.D. Landau and E.M. Lifshitz, *Fluid Mechanics* (Addison-Wesley, Reading, MA, 1989).
- [34] J. Chazy, *Bull Soc. Math., France* **52**, 17 (1924).
- [35] H.E.J Curzon, *Proc. London Math. Soc.* **23**, 477 (1924).
- [36] W.B. Bonnor, *Proc. Phys. Soc., London, Sect. A* **67**, 225 (1954).
- [37] D.M. Zipoy, *J. Math. Phys.* **7**, 1137 (1966)
- [38] B.H. Voorhees, *Phys. Rev. D* **2**, 2119 (1970)
- [39] H. Weyl, *Ann. Phys. (Leipzig)* **54**, 117 (1917)
- [40] H. Weyl, *Ann. Phys. (Leipzig)* **59**, 185 (1919)
- [41] K. Schwarzschild, *Sitzungsber. K. Preuss. Akad. Wiss.* **1916**, 189 (1916).
- [42] W.B. Bonnor, *Z. Phys.* **161**, 439 (1961).
- [43] W.B. Bonnor, *Z. Phys.* **190**, 444 (1966).

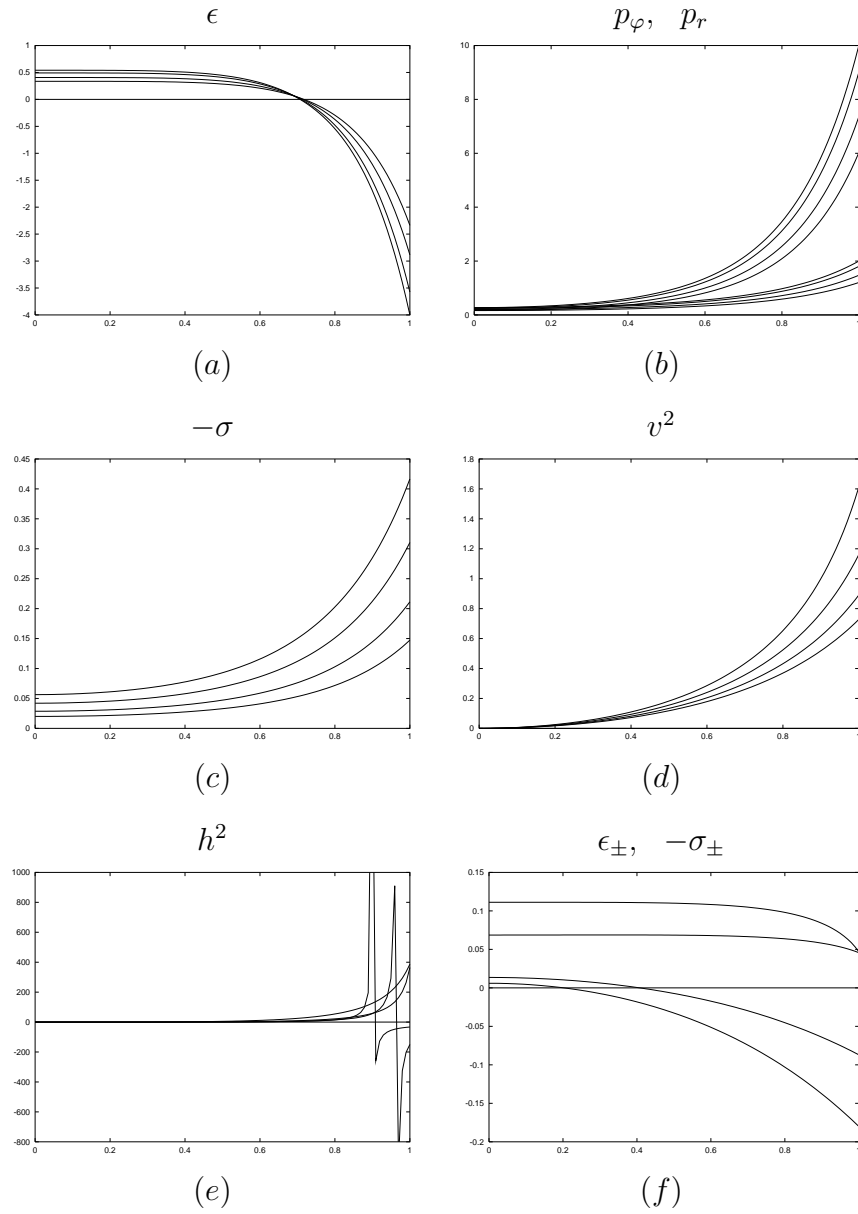


**Figure 1.** For Chazy-Curzon-type fields we plot, as functions of  $r$ , (a) the energy density  $\epsilon$  and (b) the pressures  $p_\varphi$  (upper curves) and  $p_r$  for discs with  $\gamma = 2$  and  $q_1 = q_2 = 0$  (top curves), 0.5, 1.0, and 1.5 (bottom curves), (c) the electric charge density  $\sigma$  for discs with  $\gamma = 2$  and  $q_1 = q_2 = 0$  (axis  $r$ ), 0.2, 0.3, 0.5, and 1.5 (top curve), (d)  $v^2$  for discs with  $\gamma = 0.7$  and  $q_1 = q_2 = 2$  (top curve), 3, 5, and 10 (bottom curve), (e) the angular momentum  $h^2$  for discs with  $\gamma = 0.7$  and  $q_1 = q_2 = 2, 3$  (sharp curves), 5, and 10 (top curve), and (f)  $\epsilon_\pm$  (lower curves) and  $\sigma_\pm$  for discs with  $\gamma = 0.7$  and  $q_1 = q_2 = 5$  and 10 (top and bottom curves, respectively).

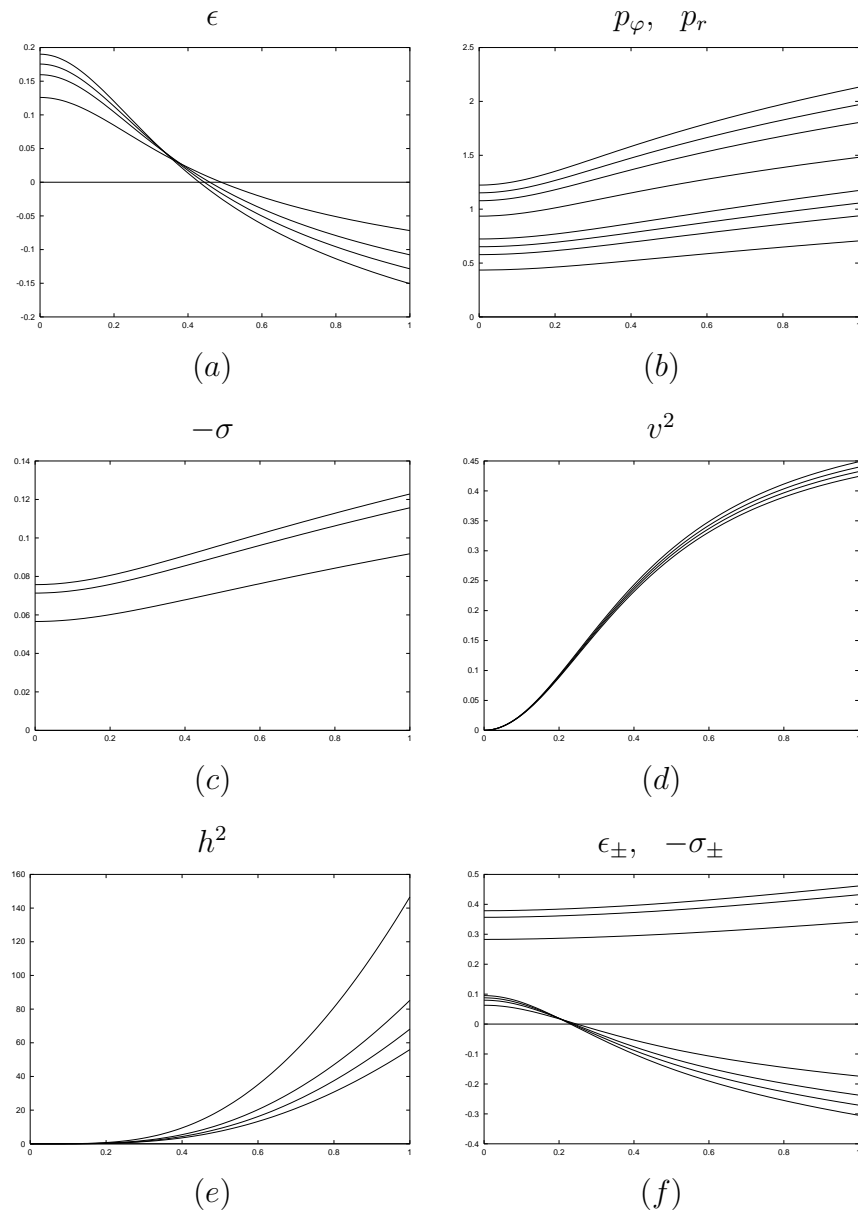


**Figure 2.** For Zipoy-Voorhees-type fields we plot, as functions of  $r$ , (a) the energy density  $\epsilon$  and (b) the pressures  $p_\varphi$  (upper curves moved upwards a factor of 0.5) and  $p_r$  for discs with  $\alpha = 3$ ,  $\gamma = 1.2$  and  $q_1 = q_2 = 0$  (top curves), 0.5, 0.8, and 1.5 (bottom curves), (c) the electric charge density  $\sigma$  for discs with  $\alpha = 3$ ,  $\gamma = 1.2$  and  $q_1 = q_2 = 0$  (axis  $r$ ), 0.5, 0.8, and 1.5 (top curve), (d)  $v^2$  for discs with  $q_1 = q_2 = 0$  (top curve), 1, 2, and 5 (bottom curve), (e) the angular momentum  $h^2$ , and (f)  $\epsilon_\pm$  for discs with  $\alpha = 3$ ,  $\gamma = 1.2$ , and  $q_1 = q_2 = 0$  (bottom curves), 0.5, 0.8, and 1.5 (top curves), and  $\sigma_\pm$  (upper curves scaled by a factor of 10) for  $q_1 = q_2 = 0$  (axis  $r$ ), 0.5, 0.8, and 1.5 (top curve) and the same values de  $\alpha$  and  $\gamma$ .

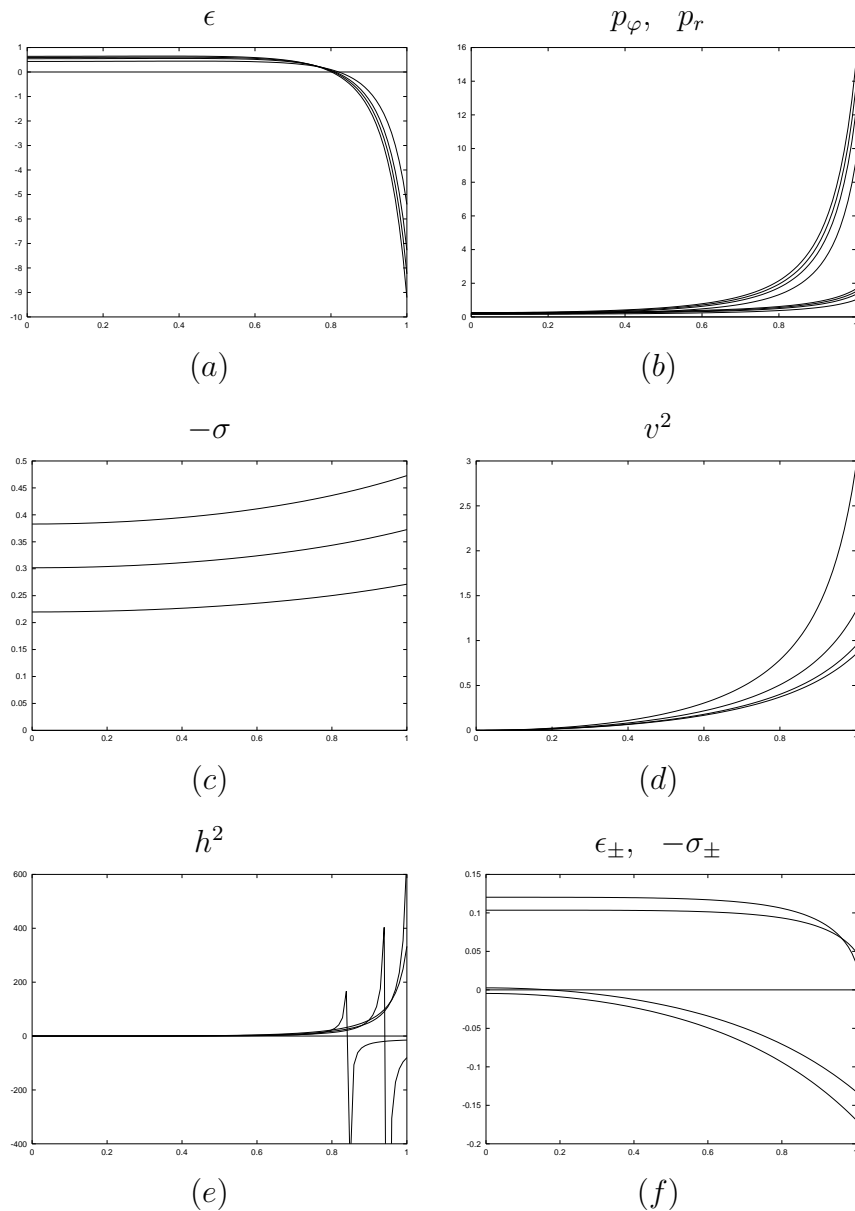


**Figure 3.** For Bonnor-Sackfield-type fields we plot, as functions of  $r$ , (a) the energy density  $\epsilon$  and (b) the pressures  $p_\varphi$  (upper curves) and  $p_r$  for discs with  $\alpha = 0.5$ ,  $\gamma = 1.3$  and  $q_1 = q_2 = 0$  (top curves), 0.5, 0.8, and 1.5 (bottom curves), (c) the electric charge density  $\sigma$  for discs with  $\alpha = 0.5$ ,  $\gamma = 1.3$  and  $q_1 = q_2 = 0$  (axis  $r$ ), 0.5, 0.8, and 1.5 (top curve), (d)  $v^2$  for discs with  $\alpha = 0.9$ ,  $\gamma = 1$  and  $q_1 = q_2 = 3$  (bottom curve), 5, 8, and 10 (top curve), (e) the angular momentum  $h^2$  for discs with  $\alpha = 0.9$ ,  $\gamma = 1$ , and  $q_1 = q_2 = 3, 5$  (sharp curves), 8, and 10 (bottom curve), and (f)  $\epsilon_\pm$  (lower curves) and  $\sigma_\pm$  for discs with  $\alpha = 0.9$ ,  $\gamma = 1$ , and  $q_1 = q_2 = 8$  and 10 (top and bottom curves, respectively).

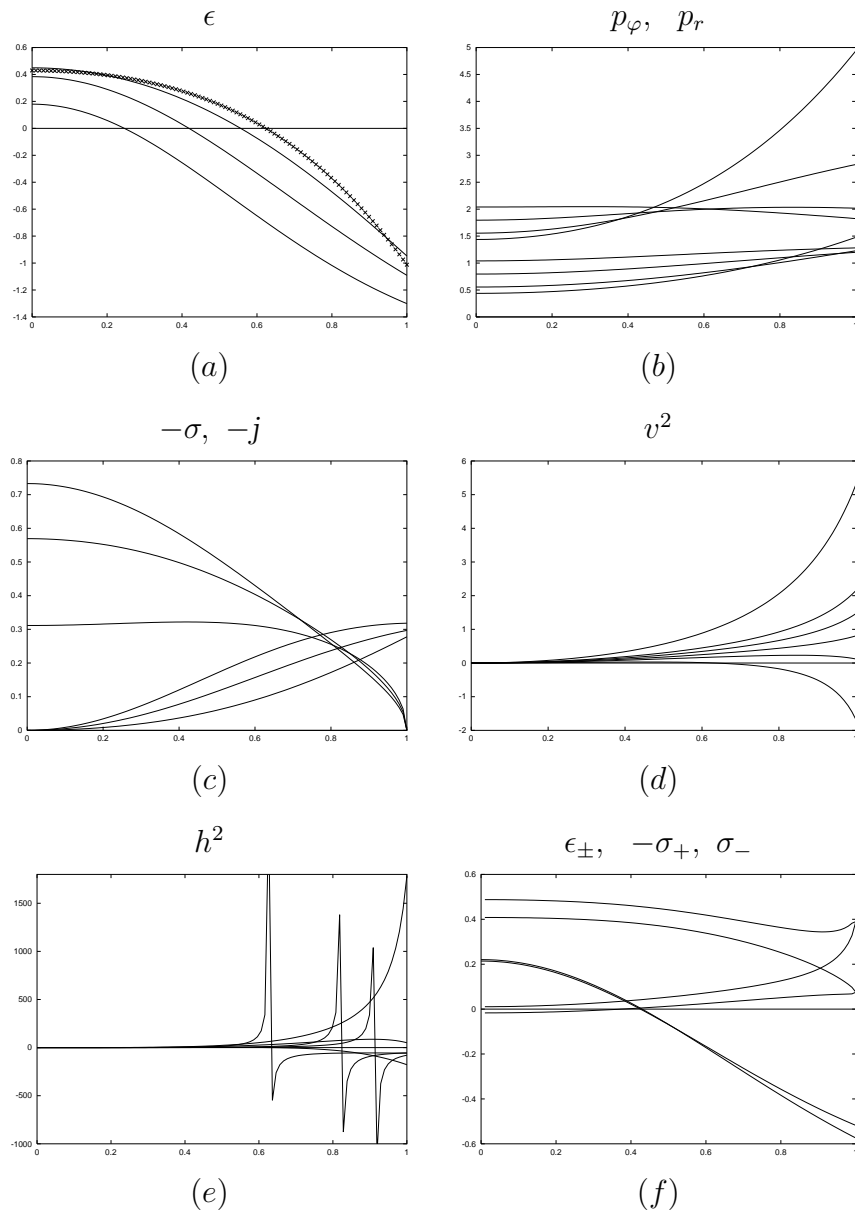


**Figure 4.** For charged and magnetized Darmois fields we plot, as functions of  $r$ , (a) the energy density  $\epsilon$  for discs with  $\alpha = 1.5$  and  $q_1 = q_2 = 0$  (curve with crosses), 0.5, 1.0, and 1.5 (bottom curve), (b) the pressures  $p_\varphi$  (upper curves) and  $p_r$  for discs with  $\alpha = 1.5$  and  $q_1 = q_2 = 0, 0.5, 1.0$ , and 1.5 (top curves at the border of the discs), (c)  $\sigma$  (upper curves) and  $j$  for discs with  $\alpha = 1.5$  and  $q_1 = q_2 = 0$  (axis  $r$ ), 0.5, 1.0, and 1.5 (top curves), (d)  $v^2$  for discs with  $\alpha = 1.5$  and  $q_1 = q_2 = 0$  (top curve), 0.5, 0.6, 0.7, 0.8, and 1.0 (bottom curve), (e) the angular momentum  $h^2$  for discs with  $\alpha = 1.5$  and  $q_1 = q_2 = 0, 0.5, 0.6$  (sharp curves), 0.7 (top curve), 0.8, and 1.0 (bottom curve), where the last curves have been scaled by a factor of 20, and (f)  $\epsilon_\pm$ ,  $\sigma_+$  (upper curves), and  $\sigma_-$  (lower curves) for discs with  $\alpha = 1.5$  and  $q_1 = q_2 = 0.7$  and 0.8 (top, bottom and bottom curves, respectively).

